

Hydrodynamic Characteristics of the Surface Piercing Propeller (SPP) by Using Special Practical and Numerical Approach

Hassan Ghassemi,

Mahmoud Ghiasi

*Department of Marine Technology, Amirkabir University of Technology, Hafez Ave.,
15875-4413, Tehran, Iran. gasemi@aut.ac.ir*

ABSTRACT:

Demands of the market for the high speed marine vehicles (HSMV) are high. This is the tasks of the naval architects to design the hull and propulsion system to diminish drag, improve the propulsive efficiency, higher safety and better maneuverability. Surface Piercing Propellers (SPPs) may provide those possessions for the vehicles. Contrasts to the immersed propellers, behavior of the SPPs have susceptibility to immersed depth, Weber number and shaft inclination angle. This paper is employed a special practical and numerical method to predict the hydrodynamic characteristics of the SPP. Critical advance ratio is obtained by practical formula using Weber number and pitch ratio in the transition mode. Numerical method is employed potential based boundary element method (BEM) on the engaged surfaces. Two models of 3 and 6 bladed SPPs are selected and some results are shown.

Key words: SPP, boundary element method, hydrodynamic characteristics,

1. INTRODUCTION

Naval architects should design the marine vehicles based on the five-S possessions (stable, shipment, strength, stealth and speed) which are interested for all merchant and naval vessel's owners. Up to now, considerations to the all possibilities have been made for increasing the speed of the vessels. Surface propellers mounted close to the transom and on shafts extended aft of the transom have been proven their effectiveness on operational craft. For steering, some surface propellers are mounted on articulated shafts and others have rudders which are often located aft of the propeller. A pair of surface propellers (Figure 1) may be highest powered units demonstrated on an operational craft to date.

An SPP is a special type of supercavitating propeller which operates at partially submerged conditions. SPPs are more efficient than submerged supercavitating propellers for number of reasons which can be itemized as follows:

- Reduction of the appendage drag due to the shafts, struts, propeller hub, etc.
- Larger propeller diameter since its size is not limited by the blade tip clearance from the hull or the maximum vessel draft;
- Reduction of the blade surface friction and erosion since cavitation is replaced by ventilation;
- Generate the vertical force to obtain the optimum running trim;
- Decreasing the torque and giving the higher efficiency.[1]

Nowadays SPP are become popular for the high speed crafts for some reasons. When the speed is increased the induced hydrodynamic pressure generates on the bottom of the hull and it causes to raise the craft. Then, the resistance of the craft is diminished and it is in fully-planing mode, as shown in Figure 2. In the case of the submerged propeller, the shaft of the propeller should be more inclined, so the propeller performance diminishes. It is advantageous to use the SPPs to reach the better performance, as depicted in the Figure 3.

SPP works in the air and water during a rotation. It operates about half of the time in the air, one-third of the time is completely submerged and the rest is partly submerged (in the entry and exit phases). During the completely submerged phase only the face (pressure side) is wetted, while the back side is surrounded by an air cavity connected to the free surface. On the back side the pressure is apparently equal to the atmospheric pressure, while a large pressure acts on the face, Figure 4.

For SPP systems, efficient experimental and numerical approaches are scarce. Ferrando et al. [2][3][4][5] and [6] carried out experimental tests and obtained the effect of many parameters

(like immersion depth, axial shaft slope, Weber number, pitch ratio) on the hydrodynamic of the SPP. Pustoshny et al [9] presented the results of the development of 5-blades SPP series for fast speed boats. Experimental works on the propulsive performance of the SPP with wedge section were studied by Nozawa & Takayama [10]. Numerical point of view, Young & Kinnas presented the BEM for the analysis of supercavitating and surface-piercing propeller flows [1].

Hydrodynamic design has not so far been fully established in the SPP system. It would be necessary to use a reliable procedure in the design of such propulsion system to increase the propulsion efficiency. In an attempt to meet these needs, the present paper introduces a numerical procedure to analyze fluid flow and hydrodynamic performance. The method is potential based BEM using some empirical formulas to distinct the partial and full ventilated zones. It is applicable to calculate in the both zones by the BEM with different boundary conditions. We study the effect of some parameters on the hydrodynamic characteristics of the SPP at different operating conditions. Two propeller types have selected for the calculations and some results of the hydrodynamic characteristics are given.

2. SOME DETAIL ON MODE OF OPERATION OF THE CRAFT AND SPP

2.1. Craft operation

HSMVs have three operational modes from start-up to the end-up speed. Theses modes are displacement mode, semi-displacement (partially-planing) mode and fully-planing mode. It is also another mode between the displacement mode and partially-planing mode, namely transition mode that the craft should pass the hump condition. If the hull of the craft be well designed and also engine provides to deliver the power to the propulsor system with receiving maximum efficiency, it is possible for the vessel to pass the hump mode. Figure 2 shows an outline of the planing craft with SPP.

The behavior of the hydrodynamic resistance against volumetric Froude number ($R_T/W - F_{nV}$) of the planing craft is shown in Figure 2. At rest and lower speed ($F_{nV} < 1.2$), the planing craft resorts to buoyancy for support (displacement mode), whereas at forward speeds ($1.2 < F_{nV} < 3.5$) a combination of hydrostatic and hydrodynamic supporting forces exists (semi-displacement mode). At $F_{nV} > 3.5$ generated hydrodynamic supporting forces on an immersed hull is caused to raise the hull in the water and decrease the wetted surface and subsequently diminish the resistance.

2.2 SPP operation

SPPs operate at the interface between air and water. For this reason some peculiar phenomena have to be taken into account to describe this kind of propulsion system. First of all one has to consider that each blade, during a propeller revolution, pierces the water surface twice. When a blade enters the water it draws some air below the water level, the air quantity depending on the propeller loading. On exiting from the water a blade carries along some water which is then thrown away producing the classic spray tail that characterizes this kind of propeller.

At advance coefficients near the zero-thrust value, the amount of air that follows the blade underwater is very small and may quite be negligible, while as J decreases the air quantity increases, along with the depth to which air is drawn. In this first stage of the operating profile the air is confined at the trailing edge of the blade and this regime is called base vented. Figure 5 (zone 5) illustrates that in both of the mentioned regimes. The shape of the K_T vs. J curve is almost the same as for a conventional propeller, the same is true for K_Q .

In the base vented mode the blade itself is still fully wetted and is tag the air cavity which extends itself from the free surface to the trailing edge. As the blade proceeds in its revolution the cavity follows until a balance is reached between the buoyancy of the air and the suction of the blade. After this point the cavity stops its descent in the water and the blade proceeds quite normally.

As the propeller loading rises the suction on the back of the blade draws the fully air. The bubble increases its volume and generally remains limited by the trailing edge. For the

maximum load of the blade, some streaks of air promote at whole back side of the blade. This is the partially vented mode of operation.

A further reduction of the advance coefficients brings the propeller into an unstable condition called transition. Here, the air cavity becomes highly unstable. The back of the blade changes continuously between fully wetted, air streaked and completely dry conditions. This phenomenon is not restricted to a single value of the advance coefficient, but rather it covers over a certain range of J . In this zone K_T and K_Q values are not unique for a given advance. Actually their value can change, depend on the condition of the back of the blades. This condition is represented by zone 4 of Figure 5. For advance coefficients below the transition range the blade is fully vented, and the volume of the air cavity increases as an inverse function of the advance coefficient. This is the so-called fully vented condition. Here the shape of thrust and torque curves departs completely from that of fully submerged propellers. When an SPP is fully vented, mainly the face of the blades produces the thrust. Actually the contribution of the suction is lost, because the back of the blades is vented to the atmosphere.

In this mode of operation the air cavities attached to the back of the blades have a considerable thickness, which keeps increasing as J is lowered. In this way the interaction of the blades is very strong and the propeller is affected by a considerable cascade effect which limits both thrust and torque. This phenomenon explains the decreasing of K_T and K_Q as J decreases, and it can be observed in zone 3 of Figure 5.

At lower advance coefficients another phenomenon appears which furthermore limits the capability of the propeller to produce thrust and absorb torque. This is the inflow retardation. The air cavities are as big as to confined streaks block confined the flow of water between the blades, decreasing the mass flow through the propeller. This, in accordance with the momentum theory, reduces the thrust that the propeller can produce. Zone 2 of Figure 5 illustrates this situation.

Finally, at extremely low values of the advance coefficient (see zone 1 of Figure 5) air demand for cavity ventilation can be choked by the huge amount of spray. In this way the pressure inside the cavities is lower than atmospheric and this increases somewhat the thrust of the propeller.

3. DETERMINATION OF THE CRITICAL ADVANCE RATIO

For a conventional propeller thrust and torque coefficients are depend on the diameter, pitch, number of blades, expanded area ratio, advance coefficient, Froude number, Reynold number, cavitation number and shaft inclination angle.

$$K_{\text{Fully-immersed}} = f(Z, P/D, EAR, J, F_n, R_n, S, \Psi) \quad (1)$$

As partially submerged propellers operate at the interface between air and water, two additional parameters must be taken into account. The first one is the immersion coefficient I_T , the second one is the Weber number, which can be formulated as

$$K_{\text{Partial-immersed}} = f(Z, P/D, EAR, J, F_n, R_n, S, \Psi, I_T, W_n) \quad (2)$$

where:

$$I_T = \frac{h_r}{D}, \quad W_n = \sqrt{\frac{(nD)^2 h_r}{k}} \quad (3)$$

and k is the kinematic capillarity.

The influence of number of blades, pitch ratio, expanded area ratio and advance coefficient on the behavior of a SPP is much the same as in case of a fully immersed propeller. The same is true for the Reynolds Number. However, the hydrodynamic performance of the SP propeller have generally three zones as mentioned before, partially ventilated zone, transition zone and fully ventilating zone. Ferrando et al [3] distinguished and experimentally obtained the critical advance speed ratio by regression method as expressed by

$$J_{CR} = S \frac{P}{D} - t \frac{P}{D} e^{-uW_n} \quad (4)$$

This practical formula depends on two factors, i.e. pitch ratio and Weber number. The regression coefficients are different for each propeller types. On this work, we have determined

some approximate coefficients by trial and error [11]. Figure 6 shows that the influence of Weber number (W_n) and pitch ratio P/D on critical advance speed ratio J_{CR} . It is obtained that when the Weber number is bigger than 250 the advance ratio is constant and it means that the zone will be fully ventilated and the back side of the blade is fully air and atmospheric pressure, so only the face side of the blade is wet and high pressure and generate the thrust or torque.

4. NUMERICAL METHOD

4.1. Geometry formulae of the propeller

A fixed O - xyz Cartesian coordinate system is selected with origin at propeller hub center, (Figure 3). x -axis is directed in the downstream, z -axis is directed vertically upward and y -axis is right hand direction. Propeller is rotating with constant angular velocity ω , ($\omega = 2\pi n$) in the counter clockwise direction and the fluid is to be inviscid and incompressible and the flow is irrotational. The coordinate point $(x_{B,F}, y_{B,F}, z_{B,F})$ of the propeller surface is expressed by the following equations

$$\begin{aligned} x_{B,F} &= r \tan \eta + (S(r) + L(r)) \sin \beta_r - Y_{B,F} \cos \beta_r \\ y_{B,F} &= r \cos(\eta_{B,F} + \theta_k) \\ z_{B,F} &= r \sin(\eta_{B,F} + \theta_k) \end{aligned} \quad (5)$$

Where:

$$\begin{aligned} h_{B,F} &= [(S(r) + L(r)) \cos b_r + Y_{B,F} \sin b_r] / r \\ q_k &= 2p(k-1)/Z \quad k = 1, 2, \dots, Z \\ b_r &= \tan^{-1} \left(\frac{P_G}{2p r} \right) \end{aligned} \quad (6)$$

and r is the radius of the propeller section, η rake angle, Z number of blades, b_r geometrical pitch angle, P_G geometrical pitch, q_k index angle of blade, $S(r)$ distance from generator line to leading edge, $L(r)$ distance from generator line to trailing edge. Y_B and Y_F are the distance of the blade section at back and face sides (respectively) to the base line [11].

4.2. Boundary element method

The basic potential flow problem in an unbounded domain is briefly formulated. The fluid is assumed to be inviscid and incompressible, while the flow is assumed to be irrotational. The flow field is described by a velocity potential Φ , which satisfies the Laplace's equation within the domain,

$$\nabla^2 \Phi = \nabla^2 (f + f_{in}) = 0 \quad (7)$$

and is subject to the impermeable boundary condition on a body surface,

$$\frac{\partial \Phi}{\partial n} = \frac{\partial (f + \dot{V}_{in} \cdot \dot{X})}{\partial n} = 0 \Rightarrow \frac{\partial f}{\partial n} = -\dot{V}_{in} \cdot \dot{n} \quad (8)$$

where n denotes the outward unit normal on a body surface. The inflow velocity, \dot{V}_{in} , is the resultant velocity of the advance velocity, \dot{V}_A , and tangential velocity, $\dot{\omega} \times \dot{r}$.

A boundary integral method involving Green's function is used to solve the boundary value problem. Green's identity can be applied over a closed zone, relating values of f and its normal derivative $\partial f / \partial n$, if f is a harmonic function. The perturbation potential $f(p)$ at the field point $p(x, y, z)$ can be expressed as,

$$2pf_P = \int_S \left\{ f_q \frac{\partial}{\partial n_q} \left(\frac{1}{R(p; q)} \right) - \frac{\partial f_q}{\partial n_q} \left(\frac{1}{R(p; q)} \right) \right\} dS \quad (9)$$

q represents the source point (x, h, v) on the surface S ($S = S_B \cup S_C \cup S_F$) over which the integration is

performed, and $R(p; q)$ is the distance between p and q . Surfaces S_B , S_C and S_F are the body surface, cavity surface and free surface, respectively.

5. NUMERICAL RESULTS

Two propellers are selected for the investigation using this practical/numerical BEM. Main dimensions of the propellers are given in table 1. One propeller has 3-blades and the other one is skewed propeller with 6-blades. Figures 7 and 10 are shown the surface element of the propellers (*SSP-1* and *SPP-2*). Profile thicknesses of the propeller at various sections are shown in Figures 8 and 11.

The hydrodynamic characteristics of the *SSP-1* propeller at two conditions (i.e. partial and fully immersed) compared in Figure 9. The pitch-diameter ratio is equaled 1.6 and the immersed ratio is 1/3. As shown in the Figure, the numerical results are good agreement with the experimental data [10]. The critical advance velocity ratio J_{CR} is almost 0.9.

The other propeller (*SPP-2*) has skew and 6-bladed with new advanced sections. As mentioned, the propeller mesh and its profile sections are shown in the Figures 10 and 11. Figure 12 shows the pressure coefficient contour of face side (pressure side) of the blade at two advance ratio ($J=0.5$ and $J=0.8$). It is immersed 40% diameter of the propeller ($h_T = 0.4D$). Hydrodynamic characteristics of the *SPP-2* propeller are shown in the Figures 13 and 14 at various pitch ratios. Critical advance ratios J_{CR} are from 0.6 (at pitch ratio 0.8) to about 1 (at pitch ratio 1.6).

6. CONCLUSION

A practical and numerical method is applied to analyze the hydrodynamic characteristics of the SPP propellers. The practical approach is very effective technique to distinct the transition zone. This may useful in the definition of the boundary conditions. The behavior and trend of the hydrodynamic characteristics of the *SPP* are quantitatively and qualitatively well agreement with the experimental one.

REFERENCES

1. Young, Y.L., Kinnas, S. A.: Analysis of supercavitating and surface-piercing propeller flows via BEM, Computational Mechanics 32 (2003) 269–280.
2. Ferrando M., Scamardella A.: Surface Piercing Propellers: Testing Methodologies, Result Analysis and Comments on Open Water Characteristics, Proc. Small Craft Marine Engineering Resistance & Propulsion Symposium, pp.5-1 – 5-27. Ypsilanti: University of Michigan
3. Ferrando M. : Surface piercing propellers: state of the art, Oc. Eng. International, 1 (2), 1997, 40-49.
4. Ferrando M., Scamardella A. : Surface piercing propellers: model tests procedures and comments on related adimensional parameters, Proceedings 5th Symposium on High Speed Marine Vehicles, Capri 24-26 March 1999 .
5. Ferrando M., Viviani M., Crotti S., Cassella P., Caldarella S. : Influence of Weber number on Surface Piercing Propellers model tests scaling, Proceedings of 7th International Conference on Hydrodynamics (ICHHD), Ischia, 4-6 October 2006
6. Ferrando M., Scamardella A. Bose N. Liu P. Veitch B., : Performance of family of Surface Piercing Propellers, Royal Istitution for Naval Architects (RINA) Transactions 2002 Part A 11p.
7. Olofsson N. : Force and Flow Characteristics of a Partially Submerged Propeller, Doctoral Thesis, Goteborg: Chalmers University of Technology – Department of Naval Architecture and Ocean Engineering, 1996.
8. Achkinadze, A. S. : Supercavitating, Highly Cavitating And Surface Piercing Propellers Design, Fast2005, St. Petersburg, Russia.
9. Pustoshny, A.V., Bointsov, V., Lebedev, E.P., Stroganov, A.A. :Development of 5-blade SPP series for fast speed boat, FAST2007, September, China.
10. Nozawa, K., Takayam, N: Experimental study on propulsive performance of SPP, J. KSNJA, No. 237, March 2002.
11. Ghassemi, H.: Numerical/practical approach on the hydrodynamic performance of the SPP, Technical report no. TR-87- No.90, NDS, 2008.

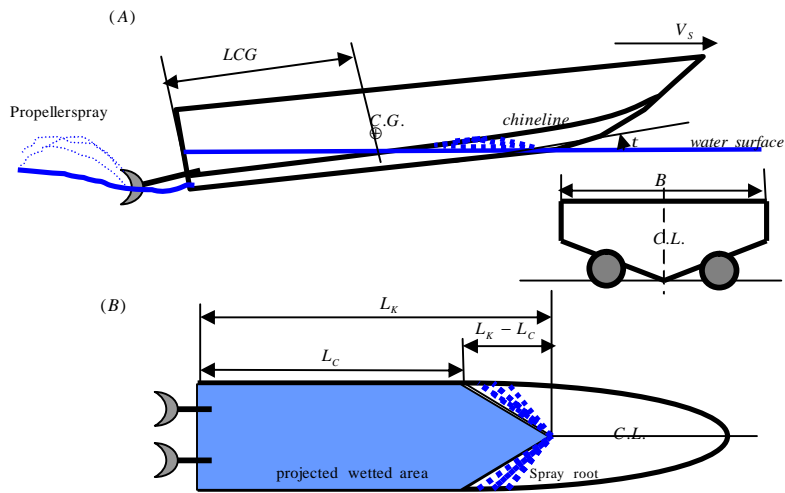


Figure 1: Outline of the planing craft with SPP

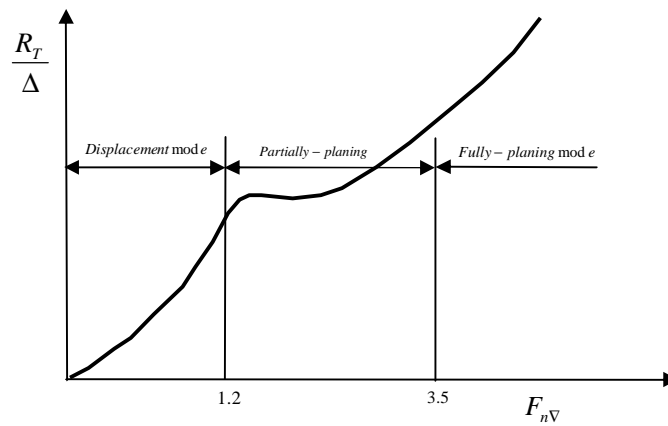


Figure 2: Behavior of the resistance/displacement vs. volumetric Froude number for a planing craft

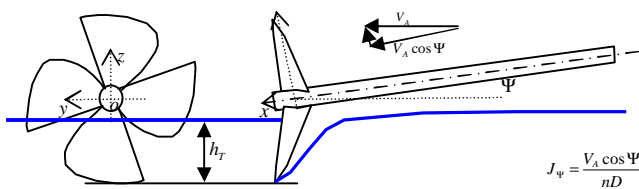


Figure 3: Coordinate system and advance velocity component

$$J_\psi = \frac{V_a \cos \Psi}{nD}$$

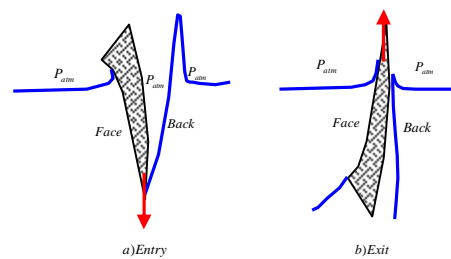


Figure 4: Propeller blade section during water entry and water exit

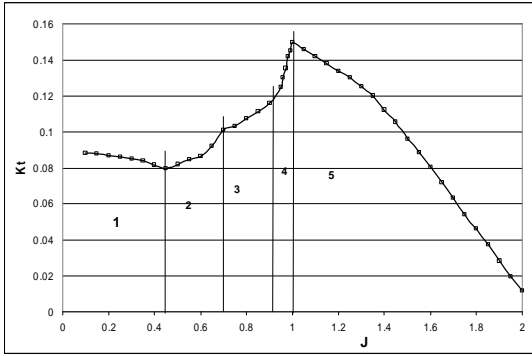


Figure 5: Trend of the thrust coefficient for SSP (instigate by Frerendo et al)

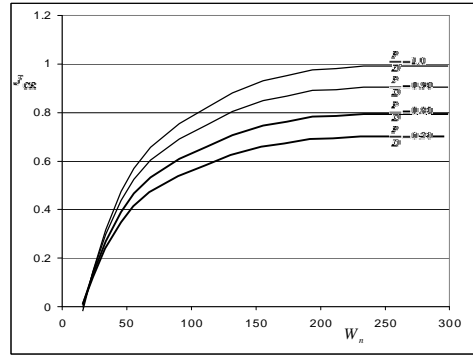


Figure 6: Predated the influence of Weber number (W_n) and pitch ratio P/D on critical advance speed ratio J_{cr}

Table 2: Main dimensions of the propellers

Propeller type	SSP-1	SSP-2
Parameters		
Diameter [m]	0.20	0.65
Boss ratio (r_h/R)	0.2	0.2
Number of blades (Z)	3	6
EAR (A_E/A_0)	0.50	0.75
Pitch Ratio at 0.7R (P/D)	1.6	Various
Skew [Deg.]	0	30.0
Rake [Deg.]	10.0	10.0
Section type	SC	Modified SC



Figure 7: Surface element of the SSP-1 propeller (two views)

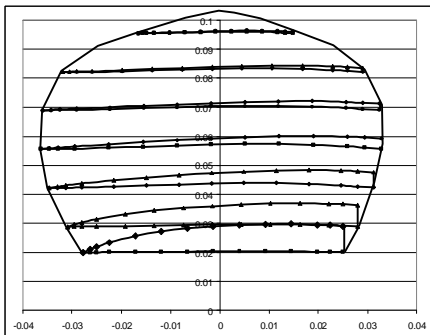


Figure 8: Profile thickness of the SSP-1 propeller

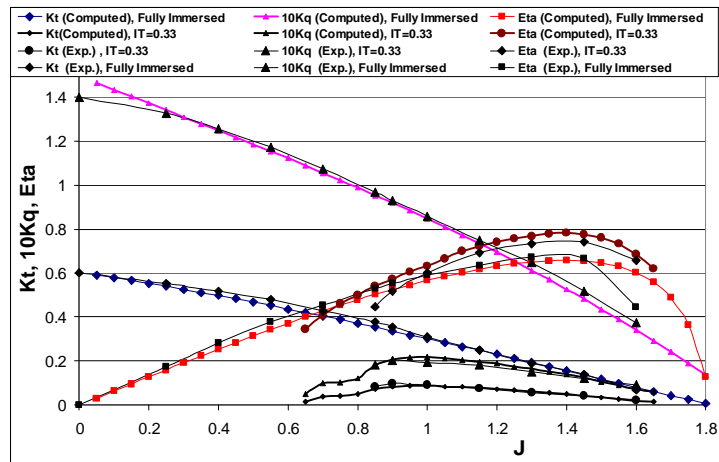


Figure 9: comparison of the hydrodynamic characteristics of the SSP-1 propeller at two partial ($I_T=h_T/D=1/3$) and immersed condition ($P/D=1.6$)

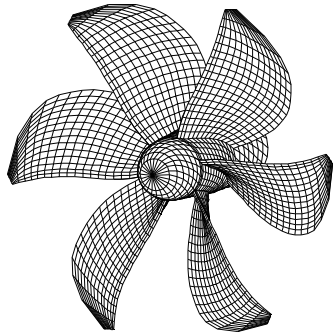


Figure 10: Surface element of the *SPP-2* Propeller

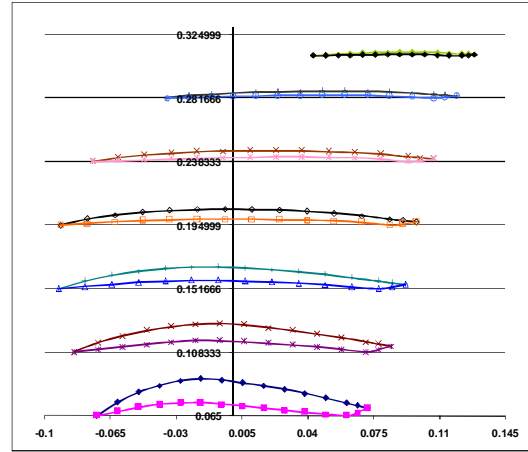


Figure 11: Profile thickness of the *SPP-2* propeller

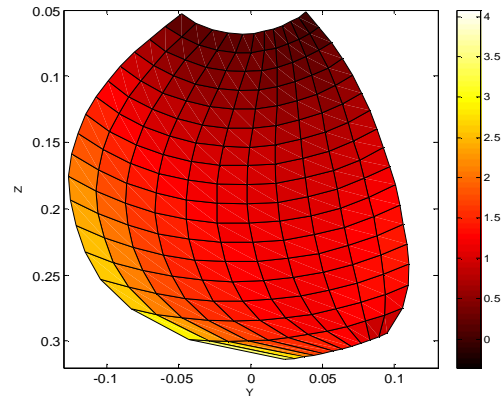
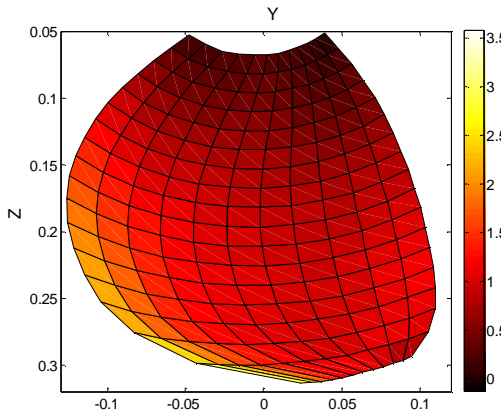


Figure 12: Pressure coefficient contour of face side of the blade of the *SPP-2* at $J=0.5$ (right) and $J=0.8$ (left), ($I_T=0.4$ and $P/d=1.6$)
(Notice: the blade is shown at vertical position, means $q = 180^\circ$)

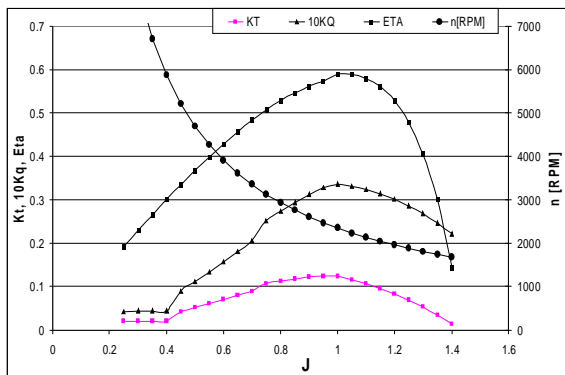


Figure 13: Hydrodynamic coefficients and rotating speed of the *SPP-2* propeller at $I_T=0.4$ and $P/D=1.6$

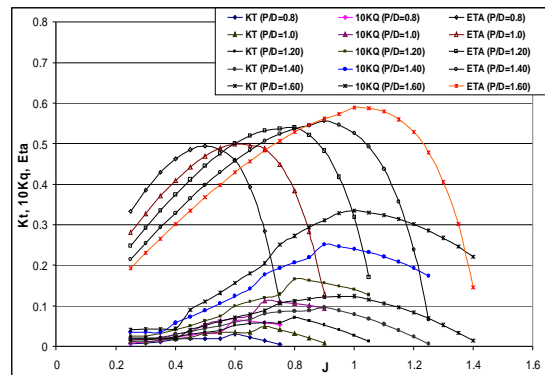


Figure 14: Hydrodynamic characteristics of *SPP-2* propeller at various pitch ratio and $I_T=0.4$